Egypt. J. Chem. **Vol. 67,** No. 4 pp. 87 - 92 (2024)

Egyptian Journal of Chemistry

http://ejchem.journals.ekb.eg/

Unveiling the morphological features of PVC/PE polymer blends: insights into improved performance

Elshod Khakberdiev,[a]* Samira Mauo,[b] Qodirbek Berdinazarov[a], Jaxongir Ibragimov[c], Nigmat Ashurov[a]

[a]*Institute of Polymer Chemistry and Physics, Academy of Sciences of the Republic of Uzbekistan, Tashkent, Uzbekistan*

[b]*Laboratoire de Chimie Appliquée, Université Mohamed-Kheider de Biskra, Biskra 07000, Algeria*

[c]*Jizzakh polytechnic institute, Jizzakh sity, Islam Karimov str 4, Jizzakh, Uzbekistan*

Abstract

This research paper explores the morphology of PVC/PE mixtures and investigates the effects of compatibilizers and mixing conditions on particle size and distribution. The study reveals that the addition of chlorinated polyethylene or graft copolymers of PVC with PE leads to smaller particle sizes and improved dispersion of the dispersed phase. These findings demonstrate the importance of compatibilizers in achieving a desirable morphology. The research also highlights the differences in morphology development between PVC-matrix and PE-matrix mixtures. In PVC-matrix blends, the compatibilizer and higher mixing speeds result in finer dispersion and uniform distribution of PE particles. Conversely, PE-matrix mixtures exhibit distinct separation into finely dispersed areas and regions with aggregated PVC particles. Overall, the study provides valuable insights into optimizing the morphology of PVC/PE mixtures, leading to improved properties. It sets the groundwork for future research on enhancing deformation characteristics through phase separation synergy and crosslinking of the PE matrix.

Keywords : chlorinated polyethylene; graft copolymers; compatibilizer; PVC; PE.

1. Introduction

The objective of polymer blending is to generate products that are economically viable with either unique characteristics or lower cost than virgin polymers. Polyvinyl chloride (PVC) that includes a proportion of polyethylene (PE) [1,2], low-density polyethylene (LDPE) [3,4], recycled low-density polyethylene (r-LDPE) [5], and high-density polyethylene (HDPE) [6,7]has been the topic of extensive studies because of the overall features of the resulting binary system.Fully immiscible polymers include PVC-PE, which has an irregular morphology, a pointed interface, and inadequate interphase adhesion [8]. Polymer blends should be compatibilized to guarantee an effective combination and development of polymer components. Several studies [9,10] have demonstrated that the most effective compatibilizers for the investigated polymer pair are chlorinated polyethylene (a copolymer of methyl methacrylate with butyl acrylate) and a copolymer of ethylene with methacrylate. To facilitate control over the morphology of this blend, an interesting concept has been proposed, which involves the dispersion of the PVC phase through the introduction of various rubbers (to lower the viscosities of the components) and a crosslinking agent for PE. As a result, the resulting morphology of the mixture exhibits a phase with trapped PVC domains within the PE content. A similar, albeit less pronounced, effect is also observed in conventional mixtures due to the simultaneous processes of macrochain breaking and crosslinking, with the ratio of these processes being determined by the oxygen concentration in the mixing medium [11,12].Adding a compatibilizer, such as PA20 or Elvaloy, can greatly improve the compatibility of PVC and LDPE

*Corresponding author e-mail: profhaqberdiyev@gmail.com; (Elshod Khakberdiev).
Receive Date: 26 July 2023, Revise Date: 25 September 2023, Accept Date: 11 October 2023
DOI: 10.21608/EJCHEM.2023.225230.8311

blends. The compatibilizer in such blends usually reacts with the other components to improve the interfacial contact between the PVC and LDPE polymers [13]. The use of anhydride maleic (MAH) as a compatibilizer to promote the interaction between immiscible polymers was also explored. [14,15]. The evolution of morphology during melt blending is another important consideration for immiscible polymer blends [16]. The absence of thermodynamic compatibility between polymer pairs at the molecular level leads to the development of a coarsely dispersed morphology, resulting in a mixture with weak interfacial adhesion. Previous studies have shown that this problem can be successfully overcome by controlling the development of the morphology during the mixing of components in a viscous-flow state [10,17,18]. Various mixing conditions, such as speed and temperature (particularly when the viscosities of the components are similar), can be employed to achieve the desired particle sizes of the dispersed phase. Stabilization of these particle sizes can be achieved by introducing compatibilizers or facilitating their formation during the mixing process. These compatibilizersare positioned at the phase boundary, preventing the coalescence of dispersed phase particles. However, apart from the PVC/PE incompatibility, the complex nature of the morphology of the mixture is also influenced by processes such as PVC dehydrochlorination, PE dehydrogenation, and the interaction of degradation products, leading to the formation of graft PVC-PE copolymers. The appearance of chlorinated PE cannot be excluded in this context. Since its beginnings in 1986, atomic force microscopy (AFM) has experienced notable development, allowing for quick and precise measurements thanks to the introduction of new cantilevers, measuring techniques, and other enhancements [19,20].

Even when measuring biological samples, AFM may achieve resolutions of roughly 1 nm, allowing for the depiction of individual atoms on flawlessly smooth surfaces [21].

Although other imaging techniques like scanning and transmission electron microscopy (SEM and TEM) may achieve comparable resolutions, AFM has the advantage of allowing the analysis of various physical and mechanical characteristics of the specimen's surface. The concept behind AFM measurements is based on the use of a cantilever with a tip to mechanically detect the surface of a sample [22]. The tip may be anywhere from 1 to 20 nm in radius and can be used in two different modes: contact mode, in which the tip moves along the sample surface, and tapping mode, in which the tip oscillates with the cantilever. Forces on the tip are approximately 10–11 N and 10– 7 N for unmodified apexes [22].

For most modes, the distance between the tip and the sample surface is between 0.1 and 10 nm. In the tapping mode, the oscillating cantilever is subject to both long- and short-range attractive and repulsive forces [23], This may improve or degrade contrast and resolution depending on the amplitude used; hence, choosing the right cantilever is crucial [24].

The same holds true for phase imaging, which is often utilized in tapping mode with topographical data. In many cases, the topographical picture is not as crisp as what is seen when the phase and amplitude of the cantilever oscillation are used [25]. However, the phase also depends on the impact hardness of the sample, the elastic properties of its surface, and the degree of adherence between the sample surface and the tip. Thus, differences in the phase can be used to differentiate between materials. AFM and nanoscale infrared spectroscopy may be used together for quantitative analysis, in which the AFM phase-imaging mode enables qualitative distinction through multiple phases [26], whereas the AFM phase imaging mode enables qualitative distinction throughout multiple phases.

Werner et al. [19] compared the results of AFM phase imaging of various FDM -printed layers to those of SEM images to determine the kind of information that can be obtained from each technique. These layers ranged fromacrylonitrile butadiene styrene(ABS) , a polymer with a well-known phase separation, to various polylactic acid (PLA) blends containing thermochromic or photochromic materials.

Based on the AFM phase pictures of ABS andthermoplastic polyurethane(TPU) blends suitable forfused filament fabrication(FFF) , de León et al. indicated that at a 10% content , TPU is evenly dispersed inside the ABS matrix, whereas at a 30% content, TPU tends to develop into a continuous phase throughout the ABS network [27]. However, there is currently a lack of reports investigating AFM phase images of both miscible and immiscible

polymer blends. This suggests the need for further research in the domain of blended materials.

Materials and methods

In this work, we used PVC suspension grade S-7059-M, TU 2212-012-466963-2008 that was manufactured by the Bashkir Soda Company Joint Stock Company (Russia, the Republic of Bashkortostan). PVC has the following physical characteristics according to Table 1. Linear low-density polyethylene (PE, ρ = 0.920 g/cm3, F-0220 brand, Shurtan gas-chemical complex of the Republic of Uzbekistan). N - dioctyl phthalate (DOP), a colourless oily liquid, was used [GOST (State Standard) 8728-88, M = 390.56 g/mol, d420 = 0.978 g/cm3]. Chlorinated polyethylene 3614A (CPE) with a chlorine content of 36 wt.% was used (Dow Chemical Co). A grafted copolymer of PE-PVC was obtained as in an earlier work [28].

Blend and composite preparation. The polymer-polymer mixtures were melt blended in a Brabender plastograph (Plasticorder Brabender OHGDUISBURG, Germany) by extrusion at a rotation speed of 50 rpm and a temperature of 180 ± 5°C for 15 min.

Table1. Specifications of PVC.

Property	Value
K value	69.7 ~ 71.5
Bulk density	0.45– 0.55
Degree of Polymerization	1250 ± 50
Particle Size	
- retained on 63 microns sieve	> 97%
- retained on 250 microns sieve	< 1%
Porosity(plasticizer absorption)	29 – 35 %
Moisture content	< 0.3%
Thermal stability	60 min at 180°C

Morphological Studies. The morphology of the polymeric mixtures was studied using atomic force microscopy (scanning probe microscope Agilent 5500) at room temperature. Silicon cantilevers with a stiffness of 9.5 N/m and a frequency of 145 kHz were used. The maximum X, Y scanning area on the AFM was 15x15 μm2, and the scanning area for Z was 1 μm.

3.Results and Discussion

Taking these factors into consideration, we analyzed experimental data regarding the morphology of a mixture of polyvinyl chloride with a linear copolymer of ethylene with butene-1 across a wide range of compositions. Due to certain limitations of atomic force microscopy, which prevents the acquisition of contrasting micrographs of surfaces with extracted dispersed phase particles, the morphology of the samples was characterized by the minimum and maximum sizes of the dispersed phase particles. The morphology parameters of the mixtures are summarized in Table 2.

Table 2. General morphology of PVC/PE polymer blends with two different speeds and two types of compatibilizer

Morphological data for the mixture PVC/PE with PVC - matrix			
№	**Composition: PVC/PE, + compatibilizer. % weight**	**Particle size of the dispersed phase, (nm)**	
		Speed mixer, 50 rpm.	**Speed mixer, 150 rpm.**
1	95/5	600 ÷ 1500, there are large aggregates (inclusions of the same size)	700 ÷ 800, uniform distribution
2	95/5/5-CPE	700 ÷ 800, slight aggregation in selection	500 ÷ 1000, uniform distribution
3	95/5/10-CPE	900 ÷ 1800, aggregated particles	600 ÷ 800, uniform distribution
4	95/5/15-CPE	500 ÷ 900, uniform distribution	400 ÷ 600, uniform distribution
Morphological data for the mixture PE/PVC with PE - matrix			
1	80/20	500 ÷ 5000, (lumps) PE mesh with PVC-domains	
2	80/20/5-CPE	500 ÷ 4000, PVC large domains - phases	200-400 ÷ 4000, large PVC domains - phases

To initiate our analysis, we will investigate blends where PVC serves as the matrix and polymer melts are generated at two distinct mixing speeds: 50 and 150 rpm.

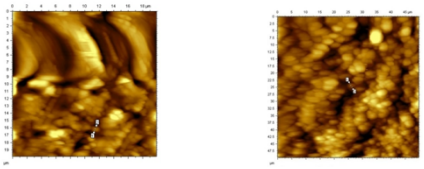

Fig. 1. PVC/PE 95/5 a) 50 rpm b) (150 rpm)

As observed in Fig. 1 and supported by the data in Table 1, in mixtures of PVC with PE, an increase in the PE content (with a mixing rate of 150 rpm) results in particles of nearly constant sizes, ranging

from 600 to 1200 nm, that are uniformly distributed within the PVC matrix. Conversely, when the mixing rate is reduced to 50 rpm, the presence of zones with aggregated particles of larger sizes is evident. This indicates the inadequate efficiency of the component mixing process in the molten state.

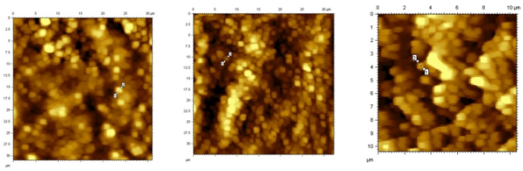

Fig. 2a. PVC/PE/CPE 95/5/5;10;15 (150 rpm)

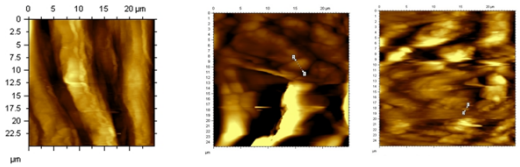

Fig. 2b. PVC/PE/CPE 95/5/5;10;15 (50 rpm)

The addition of 5-15 wt% of chlorinated PE as a compatibilizer to a PVC/PE mixture with a composition of 95/5 and mixing speeds of 50 rpm (Fig. 2a) and 150 rpm (Fig. 2b) brings about significant alterations in the size and distribution of the dispersed phase particles.

At lower mixing speeds, a coarsely dispersed morphology is maintained, with small particle sizes ranging up to several hundred nanometers. Additionally, large aggregated particles with a ribbon-like structure are observed.

Increasing the stirring speed up to 150 rpm, as determined by the equation (Ca)crit = 1/2 (16P+16)/(19P+16), results in a substantial reduction in the particle size of the dispersed phase when chlorinated polyethylene is present. In the range of CPE content at 5-15 wt%, the sizes are decreased from 700 to 400 nm (see Table 2).

A less pronounced yet similar effect is observed when a graft copolymer of PVC with PE (up to 10% wt.) is introduced. Stabilization of the particle size of the dispersed phase is also observed in compositions with high PE content, such as 90/10 and 80/20 (see Table 2).

The smallest particle sizes of the dispersed phase were observed in the PVC/PE 80/20 mixture with the addition of 10% graft copolymer (300 nm). This effect is likely attributed to the predominant localization of the compatibilizer at the phase boundary, effectively preventing the coalescence process. Additionally, an optimal concentration of the compatibilizer (20% wt.) allows for the coating of the PE-phase particles' surfaces. This effect is further enhanced by the formation of graft copolymers of PVC with short chains of PE fragments through the reaction of macroradicals from thermally degradable products of the mixture components.

The morphologies of PVC/PE blends with a polyethylene matrix are of particular interest. As mentioned earlier, the deficiency of oxygen in the mixing zones of the Brabender plastograph or in the extruder can lead to the breakage and intermolecular crosslinking of the polyethylene matrix. The micrograph in Figure 3 illustrates the presence of areas with a striped structure and PVC particles of larger sizes (over 5 μm) in the PE/PVC 80/20 composition.

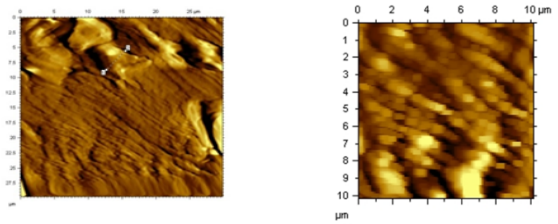

a b

PE/PVC 80/20

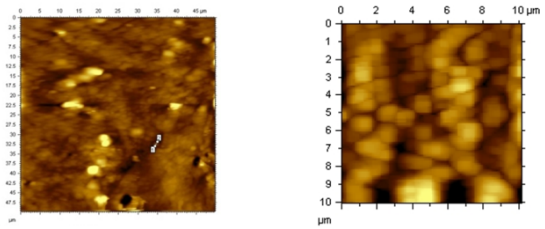

a b

PE/PVC/CPE 80/20/5

Fig. 3.Micrographs for PE/PVC 80/20 composition

The enlargement of the striped areas, which are likely composed of slightly cross-linked PE phases, allows for the identification of a finely dispersed structure within them (ranging from 500 to 1000 nm). The presence of a bulk network formed by PE phases with dispersed PVC particles serves to prevent coalescence and stabilize the morphology. Furthermore, the introduction of chlorinated polyethylene enhances the morphology, leading to a

noticeable reduction in the concentration and size of aggregates (2-3 μm).

Upon analyzing the deformation behavior of the mixtures, it can be observed that the extreme dependence of the elastic modulus at low PE contents and its location above the additive curve up to equal compositions, as well as the absence of such an effect in mixtures with a PE matrix, are consistent with the data on the morphology of the mixtures.

4. Conclusion

Based on the analysis of the morphology of PVC/PE mixtures with a PVC matrix in the presence of a compatibilizer, the following observations can be made:

Systems without a compatibilizer exhibit a thinning of the mixture morphology as the content of the PE phase increases. Along with areas containing finely dispersed PE particles, different-sized particle aggregates are also present.

The introduction of a compatibilizer and an increase in the mixing rate of the mixture components in the melt lead to further dispersion of PE particles (down to 300 nm) and their uniform distribution within the PVC matrix, without the presence of particle aggregation.

The observed formation of nanostructural morphology at low compatibilizer concentrations confirms the hypothesis of additional optimization of the compatibilizer content through the formation of a graft copolymer of PVC with PE at the phase boundary. This effect becomes more pronounced with increasing PE content in the mixture. Notably, this phenomenon is most significant for the 50/50 composition, while the difference in morphology between mixtures with and without a compatibilizer is negligible.

For mixtures with a PE matrix, the dynamics of morphology development are distinctly different. Two types of morphology can be observed: finely dispersed areas within a weakly cross-linked PE matrix and areas with aggregated PVC particles.

The concept of phase separation synergy and simultaneous crosslinking of the PE matrix, achieved through the introduction of elastomers (to ensure optimal component viscosity ratio) and a cross-linking agent (to control the density of the PE network), successfully addresses the enhancement of deformation characteristics. These approaches will be further explored in future research.

These findings provide valuable insights into the optimization and enhancement of the properties of PVC/PE mixtures, both with a PVC matrix and a PE matrix.

Conflicts of interest

The authors declare that they have no conflict of interest.

References

[1] Zevenhoven, R., Axelsen, E. P., & Hupa, M. Pyrolysis of waste-derived fuel mixtures containing PVC. Fuel. 2002; 81(4): 507-510.

[2] Bittencourt, P. R. S., & Scremin, F. R. Evolved gas analysis of PE: PVC systems thermodegradation under inert and oxidizing atmosphere. Journal of Polymers and the Environment. 2019; 27(3): 612-617.

[3] Saeedi, M., Ghasemi, I., & Karrabi, M. Thermal degradation of poly (vinyl chloride): effect of nanoclay and low density polyethylene content. Iran. Polym. J. 2011; 20: 423.

[4] Xu, C., Fang, Z., & Zhong, J. Study on phase dispersion-crosslinking synergism in binary blends of poly (vinyl chloride) with low density polyethylene. Polymer. 1997; 38(1): 155-158.

[5] Maou, S., Meftah, Y., & Meghezzi, A. Synergistic effects of metal stearate, calcium carbonate, and recycled polyethylene on thermo-mechanical behavior of polyvinylchloride. Polyolefins Journal. 2023; 10(1): 1-11.

[6] Fang, Z., Xu, C., Bao, S., & Zhao, Y. In situ crosslinking and its synergism with compatibilization in polyvinyl chloride/polyethylene blends. Polymer. 1997; 38(1): 131-133.

[7] Maou, S., Meghezzi, A., Grohens, Y., Meftah, Y., Kervoelen, A., & Magueresse, A. Effect of various chemical modifications of date palm fibers (DPFs) on the thermo-physical properties of polyvinyl chloride (PVC)–high-density polyethylene (HDPE) composites. Industrial Crops and Products. 2021; 171: 113974.

[8] Zarraga, A., Munoz, M. E., Pena, J. J., & Santamaria, A. The role of a dechlorinated PVC as compatibiliser for PVC/polyethylene blends. Polymer bulletin. 2002; 48: 283-290.

[9] Khakberdiev, E. O., Berdinazarov, Q. N. U., Toshmamatov, D. A. U., & Ashurov, N. R. Mechanical and morphological properties of poly (vinyl chloride) and linear low-density polyethylene polymer blends. Journal of Vinyl and Additive Technology. 2022; 28(3): 659-666.

[10] Prachayawarakorn, J., Khunsumled, S., Thongpin, C., Kositchaiyong, A., & Sombatsompop, N. Effects of silane and MAPE coupling agents on the properties and interfacial adhesion of wood-filled PVC/LDPE blend. Journal of Applied Polymer Science. 2008; 108(6): 3523-3530.

[11] Zhang, Y., & He, P. Properties and morphology of poly (vinyl chloride) blends with solid-state-chlorinated polyethylene. Journal of Vinyl and Additive Technology. 2010; 16(2):120-126.

[12] Yang, Z., Peng, H., Wang, W., & Liu, T. Crystallization behavior of poly (ε-caprolactone)/layered double hydroxide nanocomposites. Journal of applied polymer science. 2010; 116(5): 2658-2667.

[13] Prachayawarakorn, J., Khamsri, J., Chaochanchaikul, K., & Sombatsompop, N. Effects of compatibilizer type and rubber-wood sawdust content on the mechanical, morphological, and thermal properties of PVC/LDPE blend. Journal of applied polymer science. 2006; 102(1): 598-606.
[14] Ma, Y., Zhang, L., Du, Z., Zhao, J., Feng, Y., & Yin, J. The preparation of malefic anhydride modified polyethylene via in-situ chlorinating graft copolymerization. Polymer-Plastics Technology and Engineering. 2009; 49(1): 24-31.
[15] Maou, S., Meftah, Y., Tayefi, M., Meghezzi, A., & Grohens, Y. Preparation and performance of an immiscible PVC-HDPE blend compatibilized with maleic anhydride (MAH) via in-situ reactive extrusion. Journal of Polymer Research. 2022; 29(5): 161.
[16] Alotaibi, M. D., Alshammari, B. A., Saba, N., Alothman, O. Y., Sanjay, M. R., Almutairi, Z., & Jawaid, M. Characterization of natural fiber obtained from different parts of date palm tree (Phoenix dactylifera L.). International journal of biological macromolecules. 2019; 135: 69-76.
[17] Sombatsompop, N., Sungsanit, K., & Thongpin, C. Structural changes of PVC in PVC/LDPE melt-blends: Effects of LDPE content and number of extrusions. Polymer Engineering & Science. 2004; 44(3): 487-495.
[18] Thongpin, C., Santavitee, O., & Sombatsompop, N. Degradation mechanism and mechanical properties of PVC in PVC-PE melt blends: Effects of molecular architecture, content, and MFI of PE. Journal of Vinyl and Additive Technology. 2006; 12(3): 115-123.
[19] Werner, E., Güth, U., Brockhagen, B., Döpke, C., & Ehrmann, A. Examination of Polymer Blends by AFM Phase Images. Technologies. 2023; 11(2): 56.
[20] Giessibl, F. J. Advances in atomic force microscopy. Reviews of modern physics. 2003; 75(3): 949.
[21] Hoogenboom, B. W. Stretching the resolution limit of atomic force microscopy. Nature Structural & Molecular Biology. 2021; 28(8): 629-630.
[22] Offroy, M., Razafitianamaharavo, A., Beaussart, A., Pagnout, C., & Duval, J. F. Fast automated processing of AFM PeakForce curves to evaluate spatially resolved Young modulus and stiffness of turgescent cells. RSC advances. 2020; 10(33): 19258-19275.
[23] García, R., & San Paulo, A. Amplitude curves and operating regimes in dynamic atomic force microscopy. Ultramicroscopy. 2000; 82(1-4): 79-83.
[24] Garcia, R. P. Ruben. Dynamic atomic force microscopy methods. Surf. Sci. Rep. 2002; 47: 197-301.
[25] Joshi, J., Homburg, S. V., & Ehrmann, A. Atomic force microscopy (AFM) on biopolymers and hydrogels for biotechnological applications—Possibilities and limits. Polymers. 2022; 14(6): 1267.
[26] Zhang, J., Khanal, D., & Holl, M. M. B. Applications of AFM-IR for drug delivery vector characterization: infrared, thermal, and mechanical characterization at the nanoscale. Advanced Drug Delivery Reviews. 2022; 114646. https://doi.org/10.1016/j.addr.2022.114646
[27] De León, A. S., Domínguez-Calvo, A., & Molina, S. I. Materials with enhanced adhesive properties based on acrylonitrile-butadiene-styrene (ABS)/thermoplastic polyurethane (TPU) blends for fused filament fabrication (FFF). Materials & Design. 2019; 182: 108044.
[28] Maou, S., Meghezzi, A., Nebbache, N., & Meftah, Y. Mechanical, morphological, and thermal properties of poly (vinyl chloride)/low-density polyethylene composites filled with date palm leaf fiber. Journal of Vinyl and Additive Technology. 2019; 25(s2): 88-93.